

# Advanced Byzantine cement based composites resisting earthquake stresses: the crushed brick/lime mortars of Justinian's Hagia Sophia

A. Moropoulou<sup>a,\*</sup>, A.S. Cakmak<sup>b</sup>, G. Biscontin<sup>c</sup>, A. Bakolas<sup>a</sup>, E. Zendri<sup>c</sup>

<sup>a</sup>National Technical University of Athens, Department of Chemical Engineering, Materials Science and Engineering Section, 9, Iroon Polytechniou St., Zografou 15780, Athens, Greece

<sup>b</sup>Princeton University, Department of Civil Engineering and Operations Research, School of Engineering and Applied Science, Princeton, NJ 08544, USA

<sup>c</sup>Universita Ca' Foscari di Venezia, Dipartimento di Scienze Ambientali, Calle Larga S.Marta 2137, 30123 Venezia, Italy

Received 27 June 2000; received in revised form 16 October 2001; accepted 10 January 2002

## Abstract

Structural studies to determine the earthquake worthiness of Hagia Sophia in Istanbul have proved that the monument's static and dynamic behavior depends very strongly on the mechanical, chemical and microstructural properties of the mortars and bricks used for the masonry. Hence, the classification of the crushed brick/lime mortars under the category of advanced cement-based composites is concluded, explaining the fact that the monument still stands, as well as the very large static deformations which it has undergone, since such mortars have a very long curing period. According to the analysis of the dynamic data, the first three natural frequencies of the building were determined. These results show a decrease of approximately 5–10% in the natural frequencies, as the amplitude of the accelerations increases and returns to their initial values, due to the non-linear nature of the masonry. The above-mentioned behavior allows the structure to absorb energy without affecting irreversibly its material properties. The determination of the mortar properties indicated that they are of considerable mechanical strength and longevity. The dated mortar samples examined proved to be resistant to continuous stresses and strains due to the presence of the amorphous hydraulic formations (CSH), investigated by transmission electron microscopy (TEM) at the crushed-brick powder/binder interfaces and at a sufficient content in the binding matrix, as proved by TG-DTA, which allowed for greater energy absorption without initiations of fractures, let alone the transition of the gel to a higher order of formation. Furthermore, the interpretation of the amorphous nature of the hydraulic formations of the crushed brick/lime mortars is attempted by the experimental validation of real chemical interaction between lime and clay and the characterization of the fundamental structural units of the calcium silicate hydrates, produced by mass spectroscopy. © 2002 Elsevier Science Ltd. All rights reserved.

**Keywords:** Cement; Composites; Earthquakes; Bricks; Lime mortar

## 1. Introduction

Structural studies to determine the earthquake worthiness of Hagia Sophia in Istanbul have shown that the monument's static and dynamic behavior depends very strongly on the mechanical and chemical properties of the mortar and bricks used in its masonry [1,2].

To obtain the static deformations of the monument, it was determined that it was necessary to assume a tensile strength for the mortar of the order of 1–2 MPa, which

is many multiples of the tensile strength associated with medieval lime mortars [3]. The hydraulic nature of mortars explains, not only why the building still stands, but also the very large static deformations they have undergone, since such mortars have a very long curing period [4,5].

According to the dynamic analysis, the strong motion data from a prior 4.8 magnitude earthquake, approximately 120 km south of the building, was used to determine the first three natural frequencies of the building. These results show a decrease of approximately 5–10% in the natural frequencies as the amplitude of the accelerations increase and return to their initial values as the earthquake peters out [6]. This is due to

\*Corresponding author. Tel.: +30-1722-2119; fax: +30-1772-3215.

E-mail address: amoropul@central.ntua.gr (A. Moropoulou).

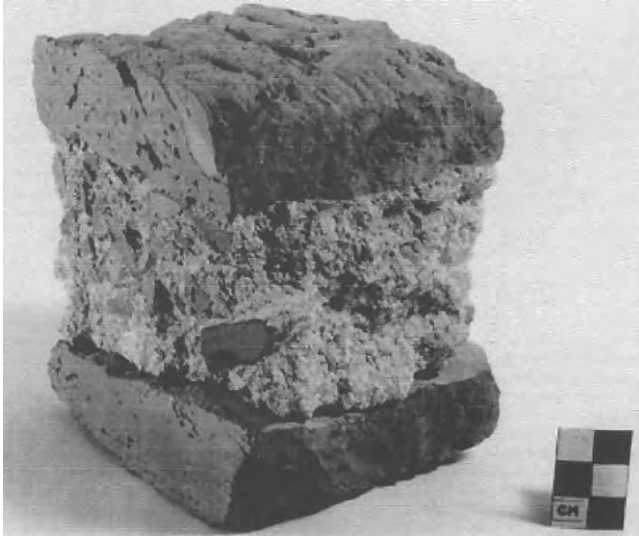


Fig. 1. Hagia Sophia mortar sample M-26 from the base of rib 7 at the west face of the main dome—dated by Van Nice to AD 558–563 (photo Dumbarton Oaks).

the non-linear nature of the masonry, rather surprising at such low levels of acceleration, indicating a type of behavior that allows for the structure to absorb energy without effecting its material properties irreversibly, which is not encountered in most modern masonry or concrete structures.

The mortars of Hagia Sophia display considerable mechanical strength along with longevity, and may be considered as early examples of reinforced concrete [7]. In fact, a typical mortar–brick sandwich sample (Fig.

1) obtained by Robert Van Nice in 1949, during a repair to a rib of the main dome of Hagia Sophia, consisting of brick building units of 5 cm and a mortar joints 1.1 times the brick thickness, was submitted to standard adhesion test at Princeton University and tensile strengths of 0.4–0.5 MPa were estimated [8].

Another sample was tested at the National Technical University of Athens (Prof Th.P. Tassios [9]) using the scratch width method with a range of tensile strength estimated to be 0.5–1.2 MPa. Two split cylinder tests on specimens approximately 40 mm long and 35 mm in diameter that were taken from the SE buttress stairwell yielded tensile strengths of 0.7 and 1.2 MPa [10].

Elastic moduli have been estimated using in-situ, ultrasonic tests at various brick and mortar locations in Hagia Sophia, including a main dome rib, the west arch, and the north arch. The estimated dynamic elastic moduli are [11]: brick:  $E_b = 3.10$  GPa; mortar:  $E_m = 0.66$  GPa; and composite:  $E_{bm} = 1.83$  GPa. These phenomena have been extensively studied in previous works, in relation either to hydraulic lime as a binder or to the crushed brick, and pozzolanic physico-chemically active aggregates, which are added in order to improve the mortar's performance [12]. In Fig. 2, which presents various traditional mortars of different processing technologies in the eastern Mediterranean Basin [13], the ratio of  $\text{CO}_2/\text{H}_2\text{O}$  bound to hydraulic components as a function of the  $\text{CO}_2$  (weight loss, %) is shown. The cement mortars are concentrated at the bottom, the crushed brick and hot lime mortars in the middle of the curve and the typical lime mortars at the upper right of ratios  $> 10$  and  $\text{CO}_2 > 32\%$ . The crushed brick mortars

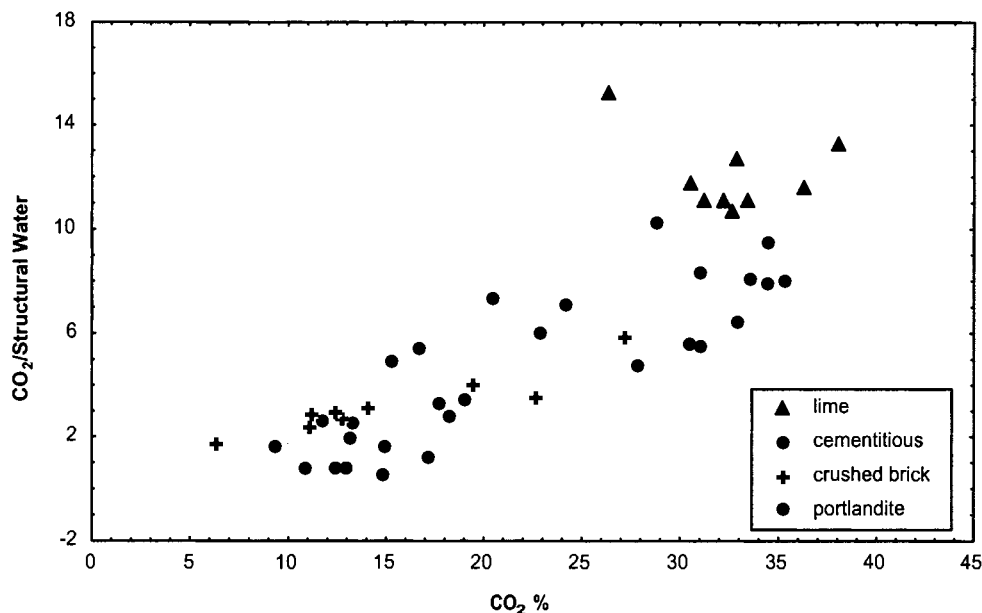


Fig. 2. Classification of traditional mortar technologies according to thermal analysis results.  $\text{CO}_2/\text{H}_2\text{O}$  structure as a function of  $\text{CO}_2$  in the Hagia Sophia mortars hydraulicity level.

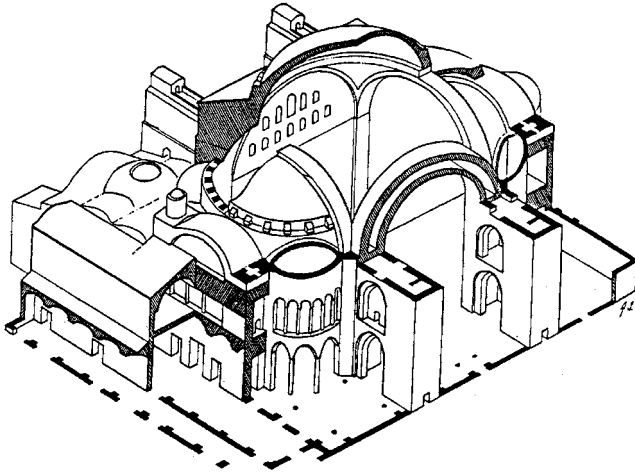


Fig. 3. Hagia Sophia main dome support structure. Sampling location. Cutaway view.

occupy a region of 2.5–7.5 along the ( $\text{CO}_2/\text{Str. water}$ ) axis vs. 10–32 along the ( $\text{CO}_2\%$ ) axis. In contrast to this, the Hagia Sophia mortars occupy the region 2.5–4 vs. 10–20, thus showing a lower calcite content and a higher hydraulic compounds content, with binder to aggregate ratios ranging from 1:4 to 1:2.

These researches have been performed within the framework of the collaboration among Princeton University (Prof A.S. Cakmak), National Technical University of Athens (Prof A. Moropoulou) and Bogazici University (Prof A. Isikara, Prof M. Erdik) [14].

The present work deals with material analyses to study the structure's ability to withstand seismic loads [14]. More specifically, the ductility of the Hagia Sophia mortars is examined in relation to the physico-chemical bonds and formations developed at the crushed brick–lime interfaces (Part I). Furthermore, the interpretation

of the amorphous nature of the hydraulic formations of the crushed brick/lime mortars is attempted by the experimental validation of real chemical interaction between lime and clay (Part II) and the characterization of the fundamental structural units of the calcium silicate hydrates, produced by NMR MAS mass spectroscopy.

## 2. Part I

### 2.1. Sampling

The primary structure supporting the main dome of the Hagia Sophia and its orientation are illustrated in a cutaway view in Fig. 3. The main dome is spherically shaped and rests on a square dome base. Major elements include the four main piers supporting the corners of the dome base and the four main arches that spring from these piers and support the edges of the dome base.

The main piers are comprised of stone masonry of almost rigid stone blocks and relatively compliant mortar, while the main arches, dome, and portions of the main piers and buttresses above it are comprised of brick masonry with thick characteristic mortar joints. Two series of mortar samples were examined. The first concerns the samples (the first five) obtained by Van Nice in 1949 and logged in at the Dumbarton Oaks Collection, Washington, DC, USA. The second concerns samples (last three) recently obtained from the monument (Table 1).

### 2.2. Experimental investigation of material properties

For the mineralogical and physico-chemical analysis, the following instrumental methods were used.

The study of the various samples starts with a detailed observation of the surface by *Fiber Optics Microscopy*

Table 1  
Sampling of mortars

| ID                                 | Location                                | Cent.             | Macroscopic description  |
|------------------------------------|---|-------------------|--|
| <i>I Samples</i>                   |   |                   |  |
| 1a                                 | From the Van Nice–Dumbarton<br>Dome Rib | Oaks<br>6th cent. | Collection<br>integral, granoblastic, crushed,<br>brick adhered to stone |
| 2                                  | Dome Rib                                | 6th cent.         | integral, granoblastic crushed<br>brick mortar                           |
| 1b                                 | West Arch                               | 10th cent.        | small pieces, friable, crushed<br>brick mortar in nodules                |
| 5a                                 | West Arch                               | 10th cent.        | small pieces, friable, fine-grained<br>crushed brick mortar              |
| 5b                                 | West Arch                               | 10th cent.        | small pieces, of friable,<br>crushed brick mortar                        |
| <i>II Sampling on the monument</i> |   |                   |  |
| 1.1                                | North-Western buttresses                | 10th cent.        | granoblastic mortar—<br>softer than the following                        |
| 2.1                                | North main Arch/west point              | 6th cent.         |  |
| 3.1                                | South-eastern abatement                 | 6th cent.         | granoblastic   |

(Keyence VH-5901) to determine the depth of adhesion and the discontinuities between the binding material and the brick fragments.

*X-Ray Diffraction Analysis (XRD)* of finely pulverized samples was performed on a Siemens D-500 X-ray diffractometer, based on an automatic adjustment and analysis system with a Diffract-EVA quality analysis software, to identify the mineral components of mortars. To facilitate the direct observation of various spectra, a *diffraction interval between 20-5 and 20-60*, with a step of 0.02 was used.

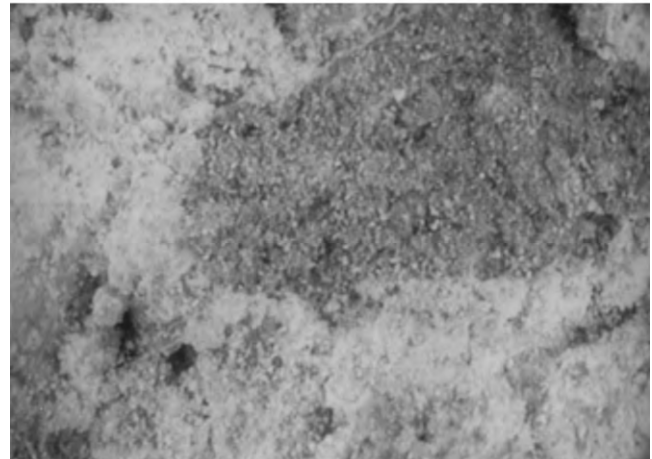
*Optical Microscopy:* Thin sections of mortar samples were examined under a polarizing Zeiss microscope. The microphotographs allow the petrographical–mineralogical characterization of the mortar constituents, as well as microscopic observations of the different mineral phases in the matrix.

*Scanning Electron Microscopy (SEM)/Energy Dispersive analysis (EDX):* Microscopic observations of the mortar samples were performed, under a scanning electron microscope (Philips 515 unit), with secondary electron emission, in order to examine the microstructure and the texture of the mortars. Energy dispersive X-ray microanalysis (elementary semi-quantitative analysis) was also performed, based on the Super Quantitative EDAX software, to determine the composition of the brick and binding materials.

A *Transmission Electron Microscope (TEM)* was used to identify amorphous phases. The measurements were performed by Mr C. Chun of Princeton University on a Philips M20/ST of Princeton Materials Institute. This procedure was used to study the nature and presence of calcium silicate hydrate (CSH) and calcium aluminate hydrate (CAH) gels of the matrix. Detection was accomplished primarily on the basis of structural and morphological characteristics of these matrix particles. TEM samples were prepared by the dipping method from colloidal suspension of particles after grinding of the mortar. After ultrasonication, the particles were suspended in methanol, and then a Cu grid coated with a holey carbon film was dipped into the suspension. After taking out the grid, it was air dried and stored for further use. The local chemical composition was preliminary examined by energy dispersive X-ray spectroscopy (EDXS), using EDAX PV9900, with a 50-nm spot size.

### 2.3. Results and discussions

Macroscopically, mortar samples 1a, 2, 2.1, 3.1 (6th c.) and 1.1 (10th c.) appear to be intact, integral and durable presenting a granoblastic character, while 1b, 1c (6th c.) and the 5a, 5b (10th c., from the West arch) are in small pieces and very friable. The ceramic fragments in the mortar are mainly reddish; some of them turn to yellow. An almost equal participation of



(a)



(b)

Fig. 4. (a,b) Fiber optics micrographs  $\times 50$ . Mortar samples a,b: 1.1.

sand and crushed brick in the mortar mixture is observed by modal analysis.

Fiber optics microscopy (Fig. 4a,b) identifies a compact microcrystalline matrix containing brick fragments of several dimensions to nodules and even powder, and several aggregates. A yellowish–pink color is observed depending on the ceramic powder dispersed and the nature of the aggregates. The reaction rims at the interface between the binding matrix and the ceramic fragments indicate strong adhesion bonds.

From the XRD results (Table 2), it is evident that the binding material of the samples is exclusively calcitic, showing slight differences as far as different aggregate fragments (quartz and plagioclase of various types) are concerned. The presence of calcium silicate hydrate (CSH) and calcium aluminate hydrate (CAH) is significant, indicating either interface reactions, or the admixture of hydraulic lime.

Observations made under a polarized microscope (Fig. 5a,b) in crossed Nikols show the reaction rims at

Table 2  
X-Ray diffraction results

| Sample      | Q    | Cc   | Ar | An | San | Do | CaAH | CaSH | Mont. | K | Muse |
|-------------|------|------|----|----|-----|----|------|------|-------|---|------|
| 2 (matrix)  | +++  | ++++ |    | ++ | ++  |    |      | +    | +     |   | +    |
| 2 (ceramic) | ++++ | ++++ |    | ++ | ++  | +  | +    | +    | +     | + | +    |
| 3 (ceramic) | ++++ | ++   |    | ++ | ++  | +  | +    |      | +     | + | +    |
| 3b (matrix) | +++  | ++++ |    | +  | +   |    | +    |      |       |   |      |

Quartz:  $\text{SiO}_2$  (5-0490); Calcite:  $\text{CaCO}_3$  (5-0586); Anorthite-plagioclase:  $\text{CaAl}_2\text{Si}_3\text{O}_8$  (12-301); Sanidine:  $\text{NaO} \cdot 6\text{KO} \cdot 4\text{ArSi}_3\text{O}_8$  (10-357); Calcium Silicate hydrate:  $5 \text{Ca}_2\text{SiO}_4 \cdot 6\text{H}_2\text{O}$  (3-0248); Calcium aluminate hydrate:  $\text{Ca}_3\text{Al}_2\text{O}_6 \cdot 8\text{H}_2\text{O}$  (2-0083); Montmorillonite:  $\text{CaNaMgFeAlSi}(\text{OH})_2 \cdot 8\text{H}_2\text{O}$ ; Kaolinite:  $\text{Al}_2\text{Si}_2\text{O}_5(\text{OH})_4$  (12-447); and Muscovite:  $(\text{K}, \text{Na})(\text{Al}, \text{Mg}, \text{Fe})_2(\text{Si}_2\text{Al})\text{O}_{10}(\text{OH})_2(7-14)$ .

the ceramic–matrix interface, dispersed in the form of veins along the matrix, filling the vacancies and discontinuities of its structure. Sample 5 gives ample evidence of these products of boundary reactions, while in sample 2, they are slightly discerned. Fine- to medium-grained aggregates of samples 5 and 2, respectively, are mainly quartz and plagioclase, varying in percentage by surface and embedded in the matrix. Careful observation of the ceramic fragments shows the presence of oxidized, very compact and more or less homogeneous ceramic pieces,

embedded by rounded fine- to medium-grained quartz and calcite.

Fig. 6a,b show reaction rims at the brick–matrix interface building up the adhesive bonds of a granoblastic compact mortar. Fig. 7 presents the electron probe microanalysis results. The matrix/brick fragment interface of samples 1a and 1b show that carbonates are substituted for calcium silicates and aluminates with simultaneous compaction of the calcite content at the

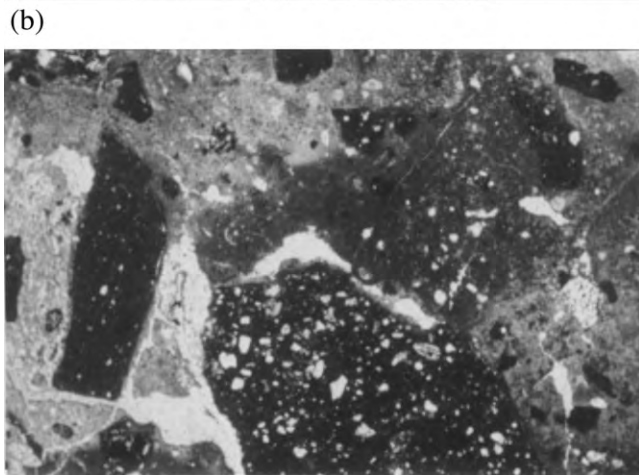
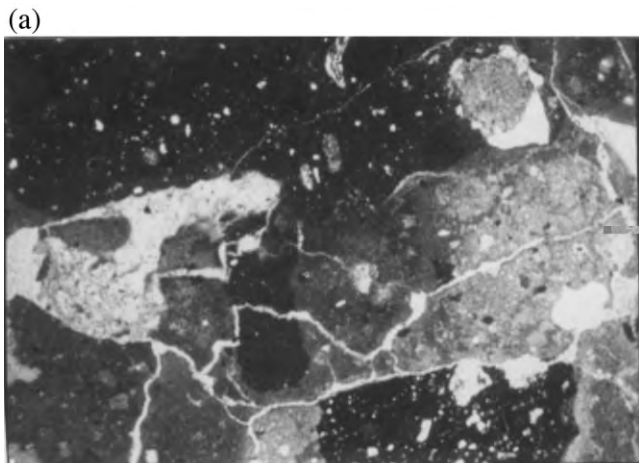
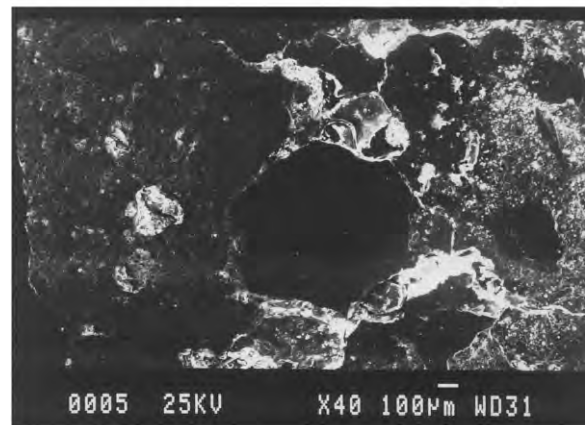
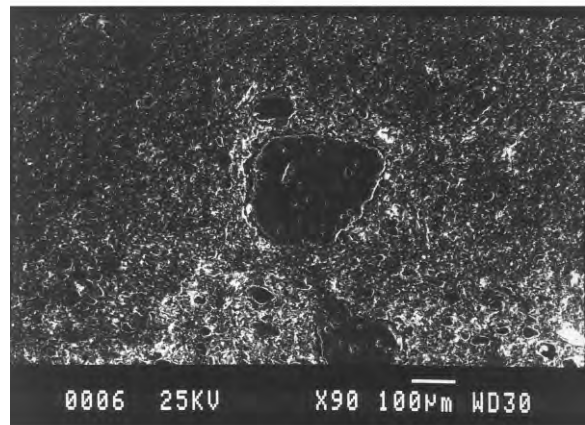


Fig. 5. (a,b) Observations under polarized microscope. (a,b) Sample 5b in crossed Nikols ( $\times 40$ ).



(a):  $\times 40$



(b):  $\times 90$

Fig. 6. (a,b) Scanning electron micrographs. Sample 2: brick fragment/matrix interface.

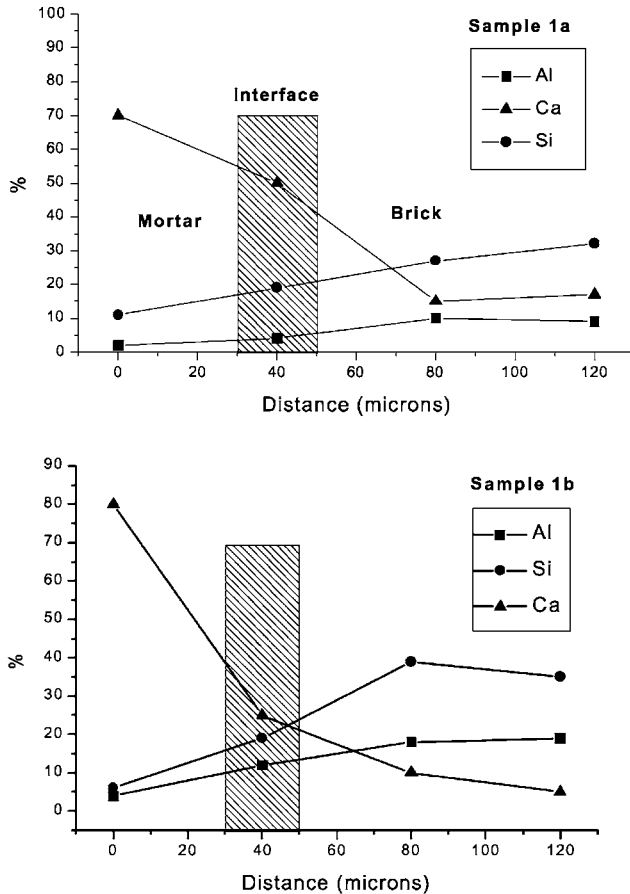


Fig. 7. (a,b) Ca, Si, Al concentration gradients (obtained by EDX measurements) at the mortar matrix/brick interface. (a) Dome rib sample 1a; (b) west arch sample 1b.

boundary [15]. The brick–mortar interface, investigated in depth over a range of 120  $\mu\text{m}$ , going from mortar to brick and considering as the interface the range 30–50  $\mu\text{m}$ , revealed the following significant features: Ca element decreases, while Si and Al species increase from mortar matrix to brick [16]. Concerning the matrix of all the specimens, a hydraulic character is revealed by the EDX measurements, due to the significant participation of Ca, Al and Si species in the binder. The binding materials of the samples 2 and 5b show a similar composition presenting high percentages of Ca (61–87%) and lower ones of Si (5.5–15%), while Al, Mg and Fe are present in low percentages. Samples 2 and 3 have similar compositions. The high percentage of Si (32–45%) and of Al (20–28%) are characteristic with a Ca percentage of 4.3–6.6%, 3.0–4.95%, respectively. Another characteristic presence is that of Fe (5.45–8.10%). The ceramics present an initial vitrification stage, most probably due to low firing temperatures. Their oxidized matrix and reddish color indicates an oxidation atmosphere in the firing kiln.

In Fig. 8, a reaction rim at the boundary surface is evidenced, where the physico-chemical penetration of  $\text{Ca}(\text{OH})_2$  to the zones immediately adjacent to the brick determines an environment of alkaline pH. In this environment, silicates could be activated [17] and the reaction product fills the discontinuities of the structure.

The dated mortar samples examined proved to be resistant to continuous stresses and strains due to the presence of the amorphous hydraulic formations (CSH), investigated by transmission electron microscopy (TEM) at the crushed-brick powder/binder interfaces and at a sufficient content in the binding matrix, as proved by TG-DTA, which allows for greater energy absorption without initiations of fractures, let alone the transition of the gel to a higher order of formation.

Fig. 9a,b shows the results obtained by transmission electron microscopy at a magnification of 22 000 (a) and 42 000 (b). The development of an amorphous C–S–H gel formation is seen between the crystalline phases of the calcite and the dispersed ceramic fragments and quartz crystals (a). In detail, the C–S–H gel presents a sheet structure (b), which in some points, gives rise to quasi-crystalline phases (b—lower left part).

### 3. Part II

#### 3.1. Materials

Depending on the temperature, the phyllosilicate minerals undergo a series of structural change [18], which may be related to the potential reaction variability of clay toward lime.

Heating the clay between 500 and 900  $^{\circ}\text{C}$  brings about fundamental transformations in the phyllosilicate

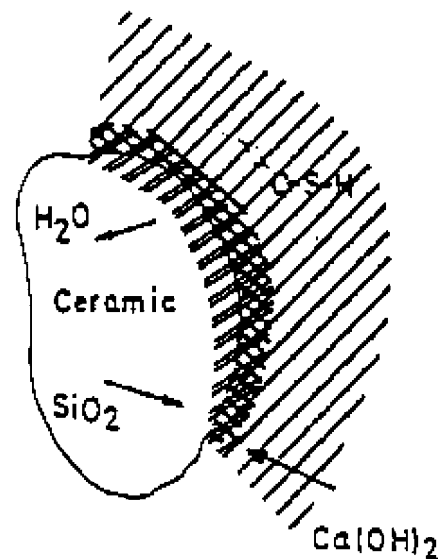


Fig. 8. Reaction ring at the mortar matrix/brick interface.

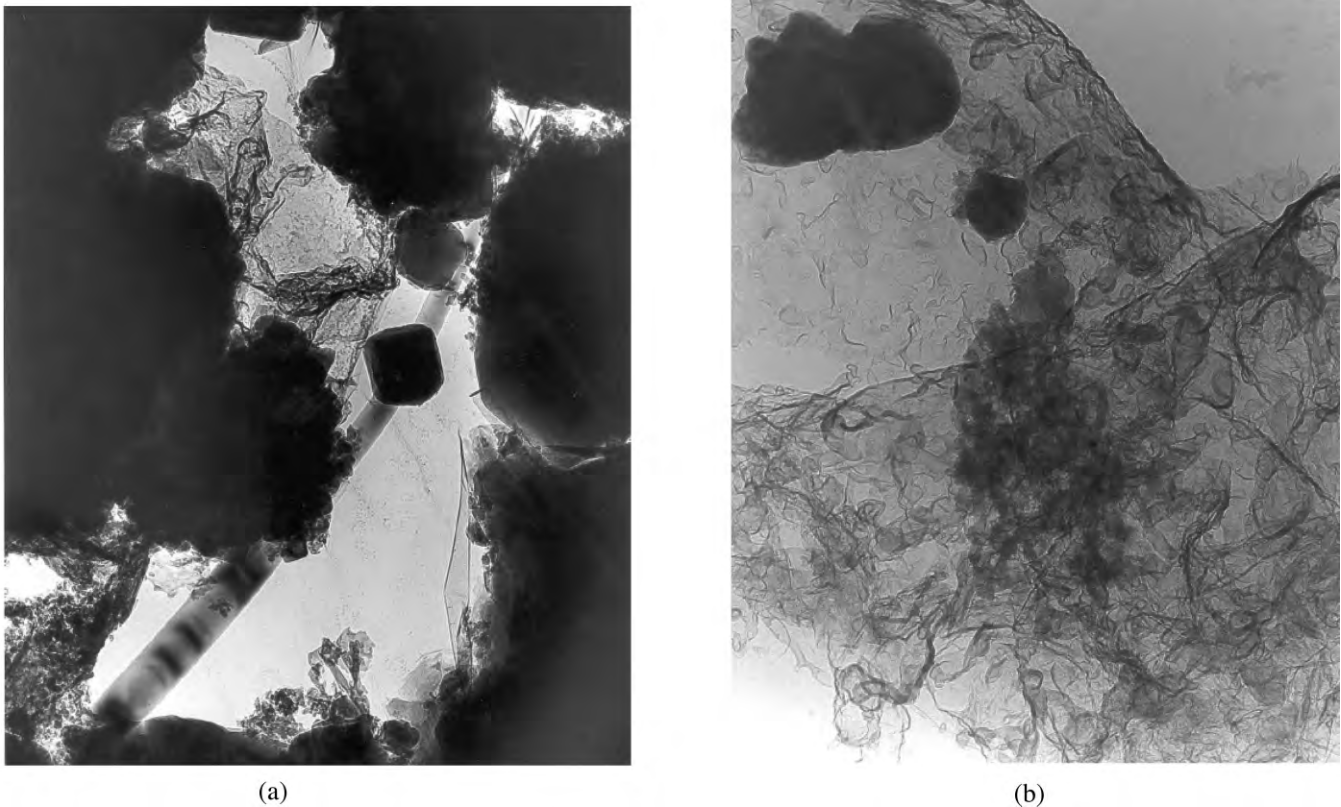


Fig. 9. Mortar sample 26—Dome rib 7: C–S–H gel crystalline interface of the calcite matrix with brick fragments. (a) 22 K magnification.

minerals, which mainly constitute conversion into an amorphous phase. This underlies the utilization of the clay samples heated in this temperature interval. In the samples of crushed brick/lime mortars manufactured and utilized in the laboratory, the brick fragments have been substituted with kaolinite rich clay. Clay samples were heated in a muffle for 24 h at 500, 550, 600, 650 and 700 °C, and then mixed in a 1:1 volume ratio with lime, utilized as lime putty containing approximately 46% water. In this first research phase, the addition of fine sand aggregates to the mixture was discarded purposely. Subsequently, the mortar samples have been preserved in the air for 5 months, under a relative humidity of approximately 60%.

### 3.2. Experimental investigation

After this period, the samples have been analyzed with  $^{29}\text{Si}$  MAS spectroscopy. The  $^{29}\text{Si}$  MAS NMR spectra were recorded on a Varian Unity 400 spectrometer operating at 79.4 MHz. A single pulse sequence was used, with quadrature detection, a pulse length of 6.0  $\mu\text{s}$ , and a relaxation delay between pulses of 60 s. For each experiment, 1600 transients were recorded, with a sample rotation frequency of 5000 rev./s. The

$^{29}\text{Si}$  spectrum of zeolite X was recorded the same day, and the spectrum of the sample was calibrated against the frequency of the most intense peak of zeolite X at  $-84.6$  ppm [19].

### 3.3. Results and discussion

The fundamental structural unit of the silicate minerals is a silicon atom surrounded by four tetrahedrally oriented oxygen atoms. The different organizations of the tetrahedra in mono-, bi-, or tri-dimensional structures can be detected with the MAS  $^{29}\text{Si}$  spectroscopy, as they give rise to different signals resonating in well-defined chemical shift intervals. More precisely, the spectroscopy allows the determination of the number of the Si–O–Si bridges for silicon atom. With four bridges, the structure extends to three dimensions, as in the case of tectosilicates (quartz or cristobalite). This structural unit is named  $Q_4$ . With three bridges, the tetrahedra form two-dimensional layers, as in the case of phyllosilicates (kaolinite, andesine, montmorillonite). This structure is named  $Q_3$ . A mono-dimensional chain is characterized by only two Si–O–Si bridges for silicon atom, and is indicated as  $Q_2$ . The single Si–O–Si bridge, which is indicated as  $Q_1$ , characterizes the dimmer or

the terminal group of a mono-dimensional chain. The  $Q_0$  term designates the single isolated tetrahedron, lacking any bond with other groups. The structural units of the  $Q_4$ ,  $Q_3$ ,  $Q_2$ ,  $Q_1$  and  $Q_0$  groups are reported together with the typical  $^{29}\text{Si}$  resonance intervals.

$^{29}\text{Si}$  MAS spectroscopy, frequently applied in the investigation of silicates, is utilized here for the first time in this area of Cultural Heritage. The obtainment of reliable results requires a careful elaboration of the MAS spectra, where the exact estimate of the relative abundance of the species is gained via the deconvolution of the often-overlapping signals into Lorentzian functions.

The  $^{29}\text{Si}$  MAS spectra of crude and of heated clay, untreated and after 5 months treatment with lime, shows the peak arrangements related to various conversions of phyllosilicates from the crystalline to the amorphous phase between  $Q_{1-4}$  structures [20,21].

A rationale of the clay–lime reactivity may be offered by the following considerations: (i) the tri-dimensional  $Q_4$  tectosilicates are not attacked by lime. (ii) The attack occurs on the bi-dimensional  $Q_3$  phyllosilicates, poorly on the  $Q_{3\text{cr}}$  structures in the crystalline state, and more efficiently in the  $Q_{3\text{am}}$  structures in the amorphous state. Thus, in the non-heated clay where the phyllosilicates are present exclusively in the crystalline form, the 5-month action of lime brings about only a scantily detectable conversion into linear  $Q_2$  silicates. Heating converts the crystalline  $Q_{3\text{cr}}$  phyllosilicates into the amorphous  $Q_{3\text{am}}$  silicates, which are more amenable to lime attack. On clay heated to 500 °C, the 5-month action of lime converts approximately 40% of  $Q_{3\text{cr}}$  and 18% of  $Q_{3\text{am}}$ . The rupture by lime of the  $Q_3$  silicon layers should mainly generate amorphous  $Q_2$  chains (Scheme 1). The small but detectable  $Q_{2\text{cr}}$  peak at –85.5 ppm may be generated by the attack of lime to  $Q_{3\text{cr}}$  silicate with retention of some crystalline order. (iii) As clays heated at 550 and 600 °C show the greatest amount of  $Q_{3\text{am}}$ , the action of lime generates the greatest amount of linear  $Q_{2\text{am}}$  form with precisely these clays.

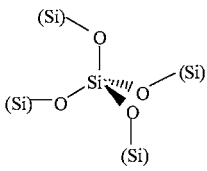
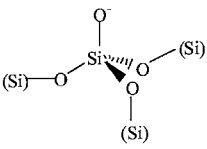
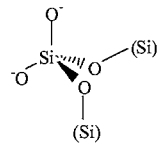
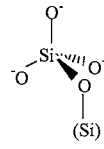
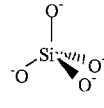
#### 4. Concluding remarks

The results and interpretation of the various analytical techniques and instrumental examinations concerning the crushed brick/lime mortars of Hagia Sophia, lead to the following conclusions: the examined mortars from the several characteristic historic periods of the building present various production technologies with binder/aggregate ratios estimated per volume from 1:4 to 1:2. Most probably, weathering, which washes out calcite, accounts for ‘low’ ratios like 1:4, not necessarily purposely implying ‘poor’ Byzantine lime process technologies. However, 1:3 could be selected as the proper mixture ratio for restoration syntheses, since it matches

with technologies of homologous mortars coming from classical and Byzantine monuments in Rhodes and Crete [22], in comparison to the lime rich 1:2 of the Ottoman period.

Nevertheless, up to now and especially when the historic composites under study concern ‘disturbed’ systems as in ‘service’ for decades of centuries under severe environmental loading, analytical techniques cannot provide direct technology information, let alone on the physico-chemical interactions, which develop the adhesion bonds among the constituents of the composite, i.e. crushed brick and lime. The binder which comprises the mortar matrix presents hydraulic character attributed partially to raw materials, like marly limestones or limestones–clay mixtures employed to produce lime, and partially to hydraulic compounds deriving from lime-crushed brick or nodules and powder interactions. The specific ‘pozzolanic’ character of the crushed brick/lime mortar is attributed to the adhesion reactions occurring at the ceramic–matrix interface, their nature depending both on the dimensions and type of ceramic (raw materials, clays and firing temperature) and the calcium hydrate content of the mortar. The grain and fragments size of the crushed brick influences directly its hydraulic reactivity, as well as its physico-mechanical properties. The observed reactions could probably be attributed to calcium silicate formations at the interface along the brick fragment, acting as the silicate source and membrane and the lime, which makes the interfacial surface alkaline and causes chemical reaction. The penetration of lime into the ceramic and the consequent reaction transforms the microstructure of the ceramic by transforming the pore radii into smaller pores, and augmenting the apparent density. The transformation of the pore size distribution matches with the cementitious character of the mortar matrix, imparting to the mortar high physico-chemical resistance to polluted and marine atmosphere, as well as high strength. The evaluation of the hydraulic formations is rather difficult, due to the physico-chemical conditions and the discontinuity at the crushed brick–lime interface. However, transmission electron microscopy provides, for the first time, valuable information concerning the development of an amorphous C–S–H gel formation between the crystalline phases of the calcite and the dispersed ceramic fragments in a sheet structure, which, in some points, gives rise to quasi-crystalline phases. The presence of the gel phase considers a matrix formation of an advanced cement based composite, which allows for greater energy absorption and explains the good performance of the historic composites in resisting earthquakes. The longevity of the examined historic composites is more or less related to the compatibility to the wall constituents, as far as the raw materials, the mortar production process and the physico-chemical and microstructural properties



|                | Structural Unit   | <sup>29</sup> Si Resonance Interval (ppm) |            |
|----------------|---|---|------------|
|                |   | crystalline                               | amorphous  |
| Q <sub>4</sub> |    | -107 ± -111                               |            |
| Q <sub>3</sub> |    | -93 ± -101                                | -99 ± -102 |
| Q <sub>2</sub> |    | -82 ± -91                                 | -80 ± -85  |
| Q <sub>1</sub> |   | -77 ± -82                                 |            |
| Q <sub>0</sub> |  | -66 ± -72                                 |            |

Scheme 1.

are concerned, which allows for continuous stresses and strains.

The interaction between lime and clay has been revealed through <sup>29</sup>[Si] MAS spectroscopy. Therefore, a real chemical interaction between lime, in the form of putty, and clay, which is given by the presences of the free oxygen valences saturated by Ca<sup>2+</sup> ions (Scheme 1), can be detected.

The interaction is maximized in clays, which have been subjected to heat and converted to the greatest amount of amorphous Q<sub>3</sub> layers (at 550 and 600 °C). This appears to be the structure with the greatest affinity with lime. The 5-month action of lime converts the Q<sub>3</sub> layers into amorphous Q<sub>2</sub> linear chains.

It remains to be assessed whether the peculiar hydraulic properties of crushed brick/lime mortars, are to be related to the presence of amorphous linear chains, in some way associated with calcium ions. Therefore, these mortars are to be tested, prepared from lime and clays heated in the 500–600 °C interval for the technological characteristics (mechanical strength, elasticity modulus, behavior toward the environment, adhesive properties

on brickworks, rheologic properties), which will recommend their use in the conservation and restoration of historical works.

Since the original mortars, which have deteriorated by natural weathering, salt decay and by the corrosive action of polluted atmospheres, have to be replaced, and the uncontrolled and extensive use of cement and polymer-based mortars, yield unsatisfactory results, due to the high content of soluble salts and the limited compatibility with the original components of the masonry, the recreation of the Hagia Sophia mortars was suggested, through a reverse engineering approach to simulate and ameliorate the historical ones. Already from the summer of 1999, have started pilot applications with compatible restoration mortars, simulating the historic ones as above, avoiding the common practice of cement mortar mixtures. These applications shall be evaluated not only by their performance during the recent earthquake, but also by their examination in situ with non-destructive tests, according to the Protocol Agreement, as well as the Agreement on Cultural Co-Operation between the Government of the Republic of Turkey and the Government of the Hellenic Republic [23].

## References

- [1] Cakmak AS, Davidson R, Mullen CL, Erdik M. In: Brebbia CA, Frewer RJB, editors. Structural repair and maintenance of historical buildings, III. Southampton, Boston: Computational Mechanics Publications; 1993. p. 67–84.
- [2] Cakmak AS, Moropoulou A, Mullen CA J. Soil Dynam Earthquake Eng 1995;14(9):125–33.
- [3] Moropoulou A, Bakolas A, Michailidis P, Chronopoulos M. In: Brebbia CA, Leftheris B, editors. Spanos Ch In Structural Studies of Historical Buildings, IV, 1. Southampton, Boston: Computational Mechanics Publications; 1995. p. 151–61.
- [4] Day W, Glover J. Bridge management, 2. London: Thomas Telford; 1993. p. 747–56.
- [5] Erdik M, Cakti E. Proceedings of STREMA '93; 3rd Int, Conf.; Bath: June 16–18. 1993. p. 99–114.
- [6] Findell K, Koyluoglu HU, Cakmak AS. J Soil Dynam Earthquake Eng 1993;12(1):51–9.
- [7] Livingston AR, Stutzman EP, Mark R, Erdik M. J Mater Res Soc 1992;267:721–30.
- [8] Mark R, Cakmak AS. Mechanical test of material from the Hagia Sophia dome. Dumbarton Oaks Papers; 1994. (p. 48).
- [9] Tassios, TP. National Technical University of Athens, Dpt. Civil Engineering; test report sent as personal communication to A.S. Cakmak, 1 Sep. 1993.
- [10] Genconglu T. STFA Inspection and Quality Control Research Consulting Co., Ltd., Istanbul Turkey test report as personal communication to A.S. Cakmak, 1 Sep. 1993.
- [11] Durukal E, Yuzugullu O, Beyen K. J. PACT 1995;55:221–9.
- [12] Baronio G, Binda L, Lombardini N. J. Constr Build Mater 1997;11(1):33–40.
- [13] Moropoulou A, Bakolas A, Bisbikou K. Thermochim Acta 1995;2570:743–53.
- [14] Program agreement on the Seismic Protection of the Hagia Sophia between the Bogazici University, Princeton University and National Technical University of Athens, Istanbul, Turkey, March 1994.

- [15] Biscontin G, Moropoulou A, Bertocello R, Bakolas A, Zendri E, Tondello E. In: Druzik JR, Vandiver PB, editors. *Materials issues in art and archaeology*, IV, 352. Pittsburg: Materials Research Society; 1995. p. 771–7.
- [16] Moropoulou, A. National Technical University of Athens, Dpt. Chemical Engineering; Lecture at Bogazici University, Istanbul, 17 March 1994.
- [17] Moropoulou A, Biscontin G, Bisbikou K, et al. In: Biscontin G, Mietto D, editors. *Scienza e Beni Culturali*, IX. Padova: Libreria Progetto Editore; 1993. p. 373–87.
- [18] Aliprandi G. *Principi di ceramurgia tecnologia ceramica*, Vol I. ECIG, 1975.
- [19] Lipman E, Magi M, Samoson A, Tarmak M, Engelhardt G. Investigation of the structure of zeolites by solid-state high-resolution  $^{29}\text{Si}$  NMR spectroscopy. *J Am Chem Soc* 1981;103:4992.
- [20] Grutzeck M, Benesi A, Fanning B. Silicon-29 magic angle nuclear magnetic resonance study of calcium silicate hydrates. *J Am Ceram Soc* 1989;72:665.
- [21] Cong X, Kirkpatrick RJ.  $^{29}\text{Si}$  MAS NMR study of the structure of calcium silicate hydrate. *Advn Cem Bas Mater* 1996;3:144.
- [22] Moropoulou A, Theodoraki A, Bisbikou K, Michaelidis P. In: Druzik JR, Vandiver PB, editors. *Materials Issues in Art and Archaeology*, IV, 352. Pittsburg: Materials Research Society; 1995. p. 759–69.
- [23] Agreement on Cultural Co-operation between the Government of the Republic of Turkey and the Government of the Hellenic Republic, 2000.